Available at www.sciencedirect.com

Metabolism

www.metabolismjournal.com

Relationship between glucose volume of distribution and the extracellular space: a multiple tracer study

Andrea Mari[a], Peter Thomas Zafian[b], Joana Achanfuo-Yeboah[b], Raul Cesar Camacho[b,*]

[a] Institute of Biomedical Engineering, National Research Council, 35127 Padova, Italy
[b] Department of In Vivo Pharmacology, Merck Research Laboratories, Rahway, NJ 07065, USA

ARTICLE INFO

Article history:
Received 19 January 2011
Accepted 23 March 2011

ABSTRACT

Although the use of radioisotopes in the investigation of glucose metabolism dates back more than 50 years, several relevant quantitative aspects have not been definitively determined. These include the volume of distribution (V_d) of glucose and recycling of glucose radioisotopes from liver glycogen. These problems are further complicated by methodological issues such as the following: (1) glucose tracers have different metabolic fates that may influence volume estimates, and (2) the calculation method needs to be based on physical principles to avoid some limitations of compartmental models. To address these issues, we administered boluses of an extracellular marker ([1-^{14}C]-L-glucose, 30 μCi) and 2 glucose tracers ([2-^{3}H]-D-glucose and [3-^{3}H]-D-glucose, 120 μCi of each), followed by a 1-mg glucagon bolus (in the presence of somatostatin) 245 minutes later, in conscious beagles to account for potential problems in recycling of the label through glycogen. We used modeling methods based on physical principles (circulatory model), which yield volume estimates with a clear physiological interpretation. Glucose V_d (mL/kg) were 204 ([1-^{14}C]-L-glucose), 191 ([2-^{3}H]-D-glucose), and 206 ([3-^{3}H]-D-glucose). These values were not different and correlated. The amount of recycled [3-^{3}H]-D-glucose in response to glucagon was small (~1.7% of the injected tracer dose). An additional result of this analysis is the determination of the parameters of the circulatory model in beagles for the standard [3-^{3}H]-D-glucose tracer. Using multiple tracers in beagles and calculation methods based on physical principles, we have provided direct proof that the glucose V_d equals the extracellular space in beagles under basal conditions.

1. Introduction

The study of glucose kinetics with tracers dates back more than half a century [1]. Many studies have elucidated key quantitative aspects of glucose homeostasis, not only enriching our understanding of physiology but also providing the basis for modeling methods [2-8] that are essential for both classic in vivo studies [9-11] and modern in silico approaches aimed at simulating the glucose homeostasis system [12,13].

Nevertheless, despite these numerous studies, several relevant quantitative aspects remain unresolved. One such aspect concerns the physiological identification of volume of distribution (V_d) of glucose. It is typically assumed that the V_d of glucose is the extracellular space [1]. This concept has been based on the notion that glucose is confined outside of cells by glucose transporters and that intracellular glucose concentration is negligible. This has also been inferred by the similarity of the estimates of the glucose V_d

Author contributions: A Mari designed the study, analyzed the data, and wrote the manuscript. P Zafian and J Achanfuo-Yeboah conducted the study. R Camacho designed and conducted the study, analyzed the data, and wrote the manuscript.

* *Corresponding author*. Tel.: +1 732 594 3175; fax: +1 732 594 1680.
E-mail address: raul.camacho@merck.com (R.C. Camacho).

0026-0495/$ – see front matter © 2011 Elsevier Inc. All rights reserved.
doi:10.1016/j.metabol.2011.03.017

and the extracellular space. However, to our knowledge, no study has directly addressed this assumption by direct comparison by simultaneously using a glucose tracer and an extracellular tracer. Although some multiple tracer studies do exist [14,15], none have calculated and compared the distribution spaces. The problem is further complicated by methodological issues, as glucose tracers have different metabolic fates that may influence the volume estimates. In addition, the calculation method needs to be based on physical principles to avoid some limitations that compartmental models have for calculating V_d [16]. Indeed, the uncertainties on the glucose V_d have caused some controversies in the past [8,16,17].

In this study, we have used an extracellular marker ([1-^{14}C]-L-glucose) and 2 glucose tracers ([2-^{3}H]-D-glucose and [3-^{3}H]-D-glucose) to test whether differences in recycling of the label through glycogen could affect the volume estimate. We have also used modeling methods based on physical principles, which yield volume estimates with a clear physiological interpretation.

2. Materials and methods

2.1. Animal preparation

Experiments were performed in overnight-fasted female beagles (13.2 ± 0.6 kg, n = 9) receiving Lab Diet dog chow (Purina Mills, St Louis, MO). The composition of the diet was 49% carbohydrate, 28% protein, and 23% fat based on dry weight. Animals were housed in a facility that met the American Association for the Accreditation of Laboratory Animals Care guidelines. All procedures were approved by the Merck Research Laboratories Institutional Animal Care and Use Committee. Sampling and infusion catheters were placed in the carotid artery and jugular vein, respectively, as previously described [18]. Experiments were performed after an overnight fast in conscious animals that had (1) no signs of bacterial infection, (2) a hematocrit of greater than 35%, (3) normal stools, and (4) a healthy appetite.

2.2. Experimental protocol

Basal samples were taken at –10 and 0 minute, after which [1-^{14}C]-L-glucose (30 μCi), [2-^{3}H]-D-glucose (120 μCi), and [3-^{3}H]-D-glucose (120 μCi, all high-performance liquid chromatography–purified from Perkin Elmer, Shelton, CT) were simultaneously injected into the jugular vein. 2 mL samples were then taken at 2, 4, 6, 8, 10, 15, 20, 30, 45, 60, 90, 120, 150, 180, 210, and 240 minutes. At 240 minutes, a 1–μg·kg^{-1}·min^{-1} somatostatin (Sigma, St Louis, MO) infusion was initiated and continued for the remainder of the experiment. At 245 minutes, another sample was taken, and then a 1-mg bolus of glucagon (Eli Lilly, Indianapolis, IN) was administered. Glucagon stimulates glucose production and mobilizes the [3-^{3}H]-D-glucose label reversibly accumulated in glycogen, if present. Samples were taken at 250, 255, 260, 275, and 300 minutes. All samples were collected in tubes containing sodium-EDTA and were frozen at –70°C until further analyses.

2.3. Assays

Plasma glucose was measured using the Trinder assay (Sigma). Plasma insulin and glucagon were measured by radioimmunoassay (Linco, St Charles, MO). For the determination of tracer counts, 1-mL plasma samples were first deproteinized with Ba$(OH)_2$ and $ZnSO_4$. [2-^{3}H] and [3-^{3}H] radioactivities in plasma were determined by selective enzymatic detritiation of [2-^{3}H]-D-glucose [19]. External standards of [2-^{3}H] and [3-^{3}H]-D-glucose suspended in control dog plasma were processed in parallel with each assay to calculate the degree of detritiation of each isotope during each sample plasma assay. Overall completion of detritiation of [2-^{3}H]-D-glucose was 93.4% ± 0.1%, whereas 99.3% ± 0.2% of [3-^{3}H]-D-glucose remained intact; tracer concentrations were corrected for detritiation. Samples were reconstituted in water and mixed with Ultima Gold scintillation cocktail (Perkin Elmer) and counted on a dual-channel Beckman Coulter counter (Fullerton, CA).

2.4. Modeling methods

The tracer decay curves were analyzed using the circulatory model previously described [16,20-22]. This approach has the advantage of using an essential physiological representation of the interaction between circulation and tissues coupled with a description of organ metabolism based strictly upon physical principles [16]. In the model (described in greater detail in the Appendix), the body is schematized as the feedback arrangement of the heart-lung block, including the heart chambers and the lungs, and the periphery block, which lumps together all remaining tissues. Each block is regarded as a single inlet–single outlet organ, and the blood flow through these lumped organs is the cardiac output (F). Glucose kinetics in the blocks are mathematically characterized by an *impulse response*, defined as the tracer efflux observed at the outlet after a bolus injection of a unit tracer dose into the inlet (assuming no tracer recirculation). Following bolus injection into a peripheral vein of the body, the tracer disappearance curve in the artery is the result of the feedback interaction of the impulse responses of the 2 interconnected blocks. To resolve the model, the following assumptions were made: (*a*) Cardiac output was assumed to be 120 mL·kg^{-1}·min^{-1}; this value was corrected for the ratio of whole-blood to plasma glucose concentration (0.73), as glucose was measured in plasma [21]. (*b*) The impulse response of the heart-lung block was assumed to be known and was represented by a 2-exponential function starting from zero and returning to zero after rising to an early peak. The parameters of the heart-lung impulse response were set to match experimentally derived curves as detailed in McGuinness and Mari [21]. (*c*) The impulse response of the periphery block [$r_{per}(t)$] was represented as a 4-exponential function, starting from zero and gradually returning to zero after reaching a peak, according to the equation:

$$r_{per}(t) = \gamma e^{-\gamma t} \otimes \left[w_1\lambda_1 e^{-\lambda_1 t} + w_2\lambda_2 e^{-\lambda_2 t} + (1 - w_1 - w_2)\lambda_3 e^{-\lambda_3 t}\right](1 - E). \quad (1)$$

In this expression, $r_{per}(t)$ is obtained as a convolution (⊗ is the convolution operator) of a 3-exponential function (in square brackets) and the single-exponential function $\gamma e^{-\gamma t}$,

which determines the fastest rising exponential term with γ = 10 min^{-1} fixed [21].

The parameter w_i (dimensionless) represents the relative weight of the exponential terms of exponent λ_I (min^{-1}), whereas E (dimensionless or %) is the glucose fractional extraction of the periphery block. Glucose clearance was calculated as $F{\cdot}E$ and the mean artery-vein transit time of the periphery block, T, from the parameters of Eq. (1) (Appendix). The equation for the volume of each block is as follows:

$$V = V_R + V_{NR} = F(1-E)T + F{\cdot}E{\cdot}\overline{T} = V_R\left(1 + \frac{E}{1-E}\frac{\overline{T}}{T}\right), \quad (2)$$

where the total volume V, precisely defined as the total mass at steady state normalized to arterial concentration, is expressed as the sum of 2 terms. The first term (V_R) is denoted as recirculating volume and is computable from cardiac output and the parameters of the impulse response. The second term (V_{NR}) is denoted as nonrecirculating volume because it is a fraction of the glucose mass that is removed by metabolism in the organs and does not exchange with the circulation. This term cannot be computed because it involves the mean artery-uptake transit time $\overline{T}$, which cannot be determined [16]. Therefore, the computable recirculating volume component was calculated (adding up the heart-lung and periphery terms) and presented in the results. Of note is that V_R and glucose clearance are dependent on integral properties of the tracer disappearance curves and coincide with the so-called noncompartmental estimates [16]. Therefore, their calculation is not particularly sensitive to the assumption of cardiac output and the details of the impulse responses (exponents and coefficients in Eq. [1]).

The model parameters were estimated from the tracer decay curves (from the tracer bolus injection to the last time point before the glucagon bolus, 0-240 minutes) using standard weighted least square algorithms. Weights were chosen to reflect an empirical estimate of the variance of the measurement error. Model residuals were computed as the difference between the measured and the model-predicted values. Residuals were calculated for the whole experimental period. During the glucagon bolus, the residuals reflect the effect of glucagon on the mobilization of the [3-^{3}H]-D-glucose label reversibly accumulated into glycogen.

Fasting glucose production was calculated as the product of clearance and mean glucose levels. During the glucagon bolus, the rates of appearance of glucose (above the basal value) induced by glucagon injection and the release of [3-^{3}H]-D-glucose from glycogen were calculated by deconvolution using the increment over basal of glucose concentration and the [3-^{3}H]-D-glucose residual, respectively. Deconvolution was performed using the individual model parameters for [3-^{3}H]-D-glucose and therefore assumed a constant clearance. In the presence of hyperglycemia and basal insulin (ie, during the glucagon bolus), glucose clearance may have been reduced (eg, DeFronzo and Ferrannini [23]). In such cases, it is possible that rates of appearance can be overestimated.

2.5. *Statistical methods*

Results are expressed as mean ± SE (SD in Fig. 1) or as median (interquartile range) for the model parameters. The significance of the differences was tested with the signed rank test; associations were tested using the Spearman correlation coefficient (ρ) at a significance level of .05.

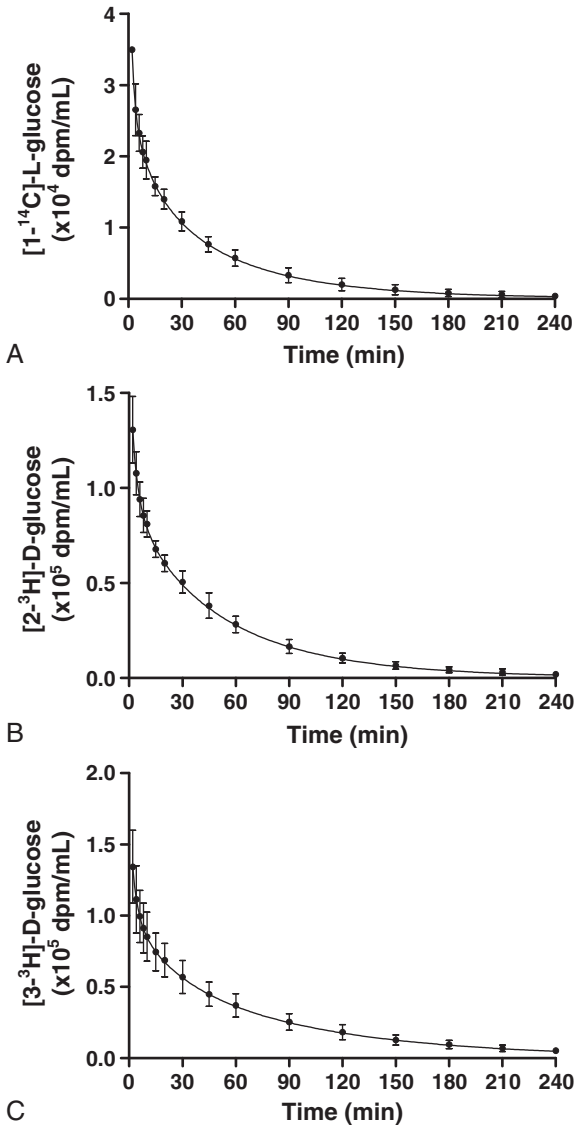

Fig. 1 – Mean (±SD) concentrations of [1-^{14}C]-L-glucose (A), [2-^{3}H]-D-glucose (B), and [3-^{3}H]-D-glucose (C), together with the model fit (solid lines). Error bars are smaller than the circle size for several points.

3. Results

3.1. *Arterial plasma glucose and insulin*

Arterial glucose remained steady throughout the experiment (1.09 ± 0.08 mg/mL) until the glucagon bolus, after which it increased to 3.69 ± 0.49 mg/mL. Arterial insulin remained constant throughout the experiment (8.5 ± 4.2 μU/mL) until the somatostatin infusion, after which it decreased to 3.7 ± 1.0 μU/mL. Arterial glucagon remained constant (55 ± 15 pg/mL) throughout the experiment until

Table 1 – Kinetic parameters of the glucose tracers

Parameter [a]	[1-^{14}C]-L-glucose	[2-^{3}H]-D-glucose	[3-^{3}H]-D-glucose
λ_1 (min^{-1})	1.85 (3.52)	1.62 (1.36)	1.17 (0.53)
λ_2 (min^{-1})	0.233 (0.095)	0.263 (0.236)	0.174 (0.074)
λ_3 (min^{-1})	0.0407 (0.0262)	0.0376 (0.0606)	0.0278 (0.0113)
W_1 (dimensionless)	0.794 (0.139)	0.797 (0.227)	0.830 (0.057)
W_2 (dimensionless)	0.182 (0.121)	0.180 (0.175)	0.147 (0.065)
E (dimensionless)	0.050 (0.009)	0.040 (0.015)	0.030 (0.008)
T (min)	2.14 (0.61)	1.99 (0.57)	2.16 (0.31)
Clearance (mL·min^{-1}·kg^{-1})	4.38 (0.82)	3.54 (1.31)	2.61 (0.68)
Volume [b] (mL/kg)	204 (54)	191 (50)	206 (27)

Results are median (interquartile range).
[a] See Eq. (1) for the symbols; cardiac output F was fixed to 120·0.73 = 87.6 mL·kg^{-1}·min^{-1} ("Modeling Methods").
[b] Recirculating volume (Eq. [2]), which includes the component of the heart-lung block (fixed to 17 mL/kg).

the glucagon bolus to mobilize all of the glycogen was given, after which it increased to above accurate limits of detection (>400 pg/mL).

3.2. *Tracer bolus analysis*

Fig. 1 shows the mean concentrations of [1-^{14}C]-L-glucose, [2-^{3}H]-D-glucose, and [3-^{3}H]-D-glucose together with the model fit. The model residuals in the period 0 to 240 minutes were randomly distributed around zero (at all time points and for all tracers, the mean residual was not different from zero by signed rank test).

Table 1 shows the mean model parameters for all tracers. As expected, [2-^{3}H]-D-glucose clearance was higher than [3-^{3}H]-D-glucose clearance (P = .0039). Glucose production was 2.86 ± 0.56 mg·kg^{-1}·min^{-1}. The recirculating volumes of all 3 tracers were not different (P = .77 by analysis of variance [ANOVA]). Both the [3-^{3}H]-D-glucose and [2-^{3}H]-D-glucose recirculating volumes were correlated with the [1-^{14}C]-L-glucose volume (ρ = 0.88, P = .0031 and ρ = 0.70, P = .043, respectively).

3.3. *Glucagon bolus analysis*

Fig. 2 shows the residuals of [1-^{14}C]-L-glucose, [2-^{3}H]-D-glucose, and [3-^{3}H]-D-glucose during the glucagon bolus and the increment from baseline of glucose concentration. Whereas [1-^{14}C]-L-glucose and [2-^{3}H]-D-glucose residuals showed little changes, a reappearance of [3-^{3}H]-D-glucose was evident from the significant increment of the concentration of this tracer (positive residual).

Fig. 3 shows the rate of appearance of glucose above the basal value and [3-^{3}H]-D-glucose after the glucagon bolus, calculated by deconvolution. The release of glucose was sustained for the whole period, whereas [3-^{3}H]-D-glucose appearance returned to zero in approximately 45 minutes. The integral of the incremental glucose appearance was 0.83 ± 0.14 g/kg, whereas that of [3-^{3}H]-D-glucose was (319 ± 88) × 10^{3} dpm/kg or approximately 1.7% of bolus dose ([184 ± 30] × 10^{5} dpm/kg).

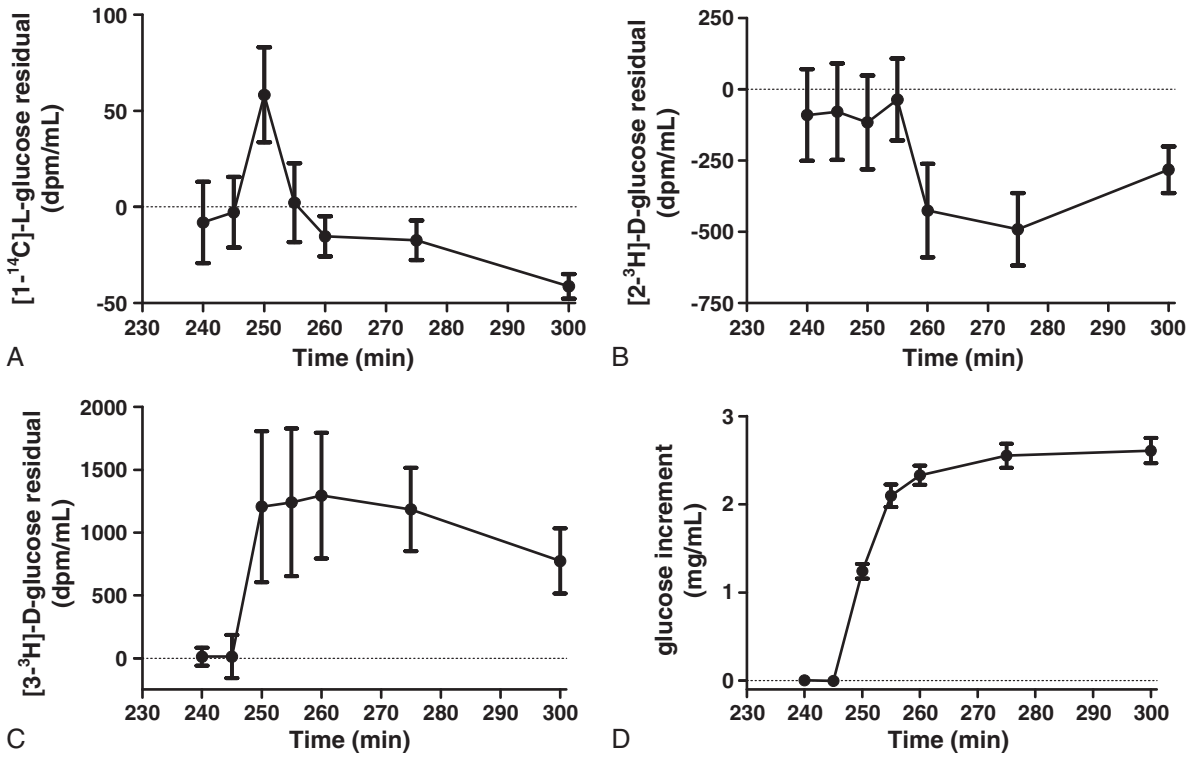

Fig. 2 – Mean (±SE) residuals of [1-^{14}C]-L-glucose (A), [2-^{3}H]-D-glucose (B), and [3-^{3}H]-D-glucose (C) and increment from baseline of glucose concentration (D) during the glucagon bolus.

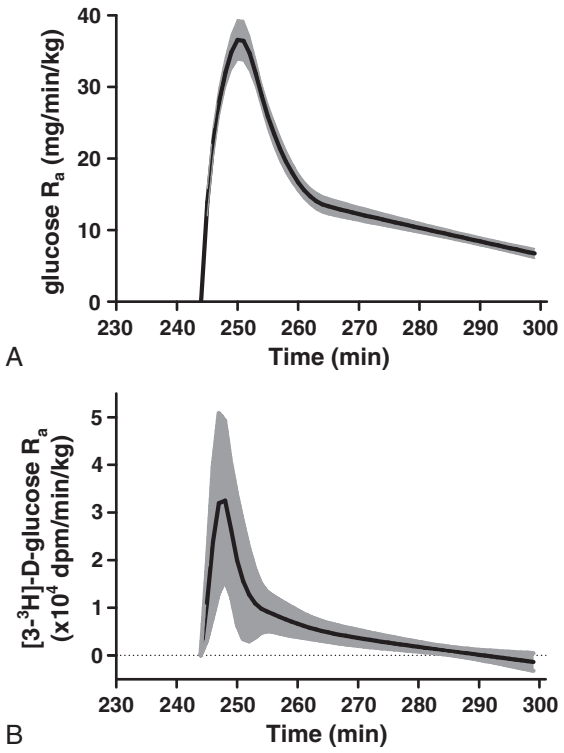

Fig. 3 – Mean (±SE, as shaded areas) rate of appearance of glucose above the basal value (A) and rate of appearance of [3-^{3}H]-D-glucose (B) after the glucagon bolus.

4. Discussion

In this study, we show that the glucose V_d equals the extracellular space in beagles in basal conditions. We have used both a multiple tracer approach and a physiologically based model for the determination of glucose V_d, an approach that has not been previously used. The extracellular marker [1-^{14}C]-L-glucose is a stereoisomer of glucose not transported by the glucose transporters [24] and thus is the extracellular marker most similar to endogenous glucose. [3-^{3}H]-D-glucose is the radioactive tracer most commonly used in the study of glucose metabolism. However, its label may be reversibly incorporated into glycogen [25], thus contributing to estimates of glucose V_d. Therefore, we also used [2-^{3}H]-D-glucose, the label of which is rapidly eliminated in the glucose-6-phospate/fructose-6-phospate reaction and diverted from the glycogen synthetic pathway. We have shown that, in agreement with previous findings, [2-^{3}H]-D-glucose does not recycle through glycogen, whereas [3-^{3}H]-D-glucose does (Fig. 2). We also have shown for the first time that the [2-^{3}H]-D-glucose and [3-^{3}H]-D-glucose volumes are equivalent. Therefore, the possible recycling of [3-^{3}H]-D-glucose through glycogen does not introduce a significant bias in the [3-^{3}H]-D-glucose V_d estimate due to a potentially slowly equilibrating glycogen pool. These findings support the conclusion that the glucose V_d and the extracellular space are equivalent.

With regard to the calculation methods for glucose V_d, we have used an approach [16,20] that is based on physical principles to avoid the potential pitfalls of the more traditional compartmental models [16]. With compartmental models, the volume estimate depends on the compartmental configuration, which requires assumptions. Because compartments do not represent physical entities, the configuration assumptions cannot be in relation to the physical processes and may lead to biased volume estimates [16].

In contrast, the circulatory model theory clarifies on physical grounds what the intrinsic limitations in the calculation of the V_d are and provides an equation for V_d that has physical foundations, although it contains undetermined quantities. In particular, the theory shows that the volume estimates are apparent volumes, as they are not a physical space but the steady-state glucose mass normalized to steady-state glucose concentration. If concentration gradients in the system are negligible, only then does this estimate represent a physical volume. Furthermore, the theory demonstrates that tracer experiments are only capable of calculating a fraction of this apparent volume, which has been denoted as "recirculating volume" and presented in Table 1. Another fraction cannot be determined because part of the glucose mass is metabolized by tissues and does not exchange with the circulation [16].

Despite these intrinsic limitations, one important advantage of the circulatory model theory is that it allows estimation of the total volume on physical grounds (Eq. [2]) based on assumptions on the undeterminable parameters. Eq. (2) shows that at small fractional extractions (such as in the current basal conditions), the difference between the recirculating and the total volumes is small, as long as the artery-uptake mean transit time is not much larger than the artery-vein mean transit time (~3% difference, from Eq. [2] assuming equality of the mean transit times, $T = \overline{T}$). Although the latter condition is not testable, large differences between the artery-vein and artery-uptake mean transit times are expected only in the presence of significant unidirectional transport barriers in the tissues that may allow accumulation of glucose in regions that do not exchange with blood. This condition is unlikely for glucose. Therefore, it seems safe to conclude that the glucose distribution space is the extracellular volume.

For our aim of determining the distribution volumes, it was logical to use a physically based approach rather than compartmental analysis for the reasons discussed above. This does not imply that compartmental models would necessarily be inappropriate for this purpose. As shown in previous studies [7,8], compartmental models can provide an adequate data fit, similar to that of Fig. 1. In addition, it is known that the V_d estimate obtained from a mammillary compartmental model with elimination from the central compartment coincides with the so-called noncompartmental volume estimate, which in turns equals the recirculating volume presented in Table 1 [16]. Therefore, as long as the data are accurately described, this compartmental model would yield a volume equivalent to that of the circulatory model. However, compartmental analysis lacks an expression of the total volume based on physical grounds such as Eq. (2).

In this work, we have applied a general use modeling approach to a specific problem. The study of the glucose distribution space in other conditions, such as the controversial

hyperinsulinemic state [8,16,17], is a possible future application. On the other hand, the circulatory model has already been used to study glucose kinetics in non–steady state, both as a general tool [22,26] and as the core to develop glucose homeostasis models [27,28]. Developments in the latter area are also of potential interest.

Concerning the non–steady-state tracer analysis method [22], an additional novel result of this study is the determination of the parameters of the circulatory model for the standard [3-^{3}H]-D-glucose tracer (Table 1) in beagles, the preferred canine model for glucose metabolism studies in the pharmaceutical industry. The mean parameters are necessary when individual parameters are not available [22,26]. The values previously reported were applicable to humans and rats only [22,28].

In conclusion, using multiple tracers in beagles and calculation methods based on physical principles, we have provided direct proof that, under basal conditions, the glucose V_d equals the extracellular space, within the intrinsic limitations of the tracer method.

Acknowledgment

We would like to thank Paul Cunningham, Gina Chevalier, Tu Trinh, and Jennyann Fischer for surgical assistance. We would also like to thank Dr Masakazu Shiota of Vanderbilt University for technical advice.

Appendix A

This appendix gives an outline of the circulatory model previously described by Mari [16,20], McGuinness and Mari [21], and Mari et al [22], using a notation similar to that used by Mari et al [22], where additional details can be found.

The mathematical description of the circulatory model is based on a multiexponential representation of the single-pass impulse response of the heart-lung and periphery blocks involved in the model. For physical reasons, the impulse response $r(t)$ starts from zero, rapidly reaches a peak, and then gradually returns to zero. In addition, the area under $r(t)$ from zero to infinite is less than 1; and 1 – area is the fractional extraction [16]. Thus, a multiexponential $r(t)$ with $N \geq 2$ exponential terms can be represented as a convolution of a single-exponential function and a multiexponential function with N – 1 terms. The expression for N = 4 is:

$$r(t) = \gamma e^{-\gamma t} \otimes \left[w_1\lambda_1 e^{-\lambda_1 t} + w_2\lambda_2 e^{-\lambda_2 t} + (1 - w_1 - w_2)\lambda_3 e^{-\lambda_3 t}\right](1 - E). \quad \text{(A1)}$$

In this expression, ⊗ is the convolution operator; and the particular representation of the exponential functions ensures the following: (1) convolution with the single-exponential function $\gamma e^{-\gamma t}$ ensures that the area under $r(t)$ equals that under the multiexponential function to the right of the convolution operator; (2) the area under the multiexponential function in square brackets is 1, as the area of each exponential term $\lambda_k e^{-\lambda_k t}$ is 1 and the coefficients (w_1, w_2, etc) add up to 1; (3) because of the previous properties, the area of $r(t)$ is 1 – E, that is, E is the fractional extraction; (4) the parameter γ of the single-exponential function determines the fast rising phase of $r(t)$; and (5) the coefficients of the exponential terms (w_1, w_2, etc) represent the relative contribution of each term to the total area.

Eq. (A1) is the equation used to describe the periphery block. Because the parameter γ has little influence on the whole-body response and cannot be determined from the data, it has been fixed to a value of 10 min^{-1} [21,22].

A 2-exponential impulse response for the heart-lung block has been used. Based on literature data, the glucose fractional extraction in heart-lung block was assumed to be negligible; and the glucose distribution volume was fixed to 17 mL/kg [21,22]. Thus, the impulse response was:

$$r_{hl}(t) = \beta e^{-\beta t} \otimes \omega e^{-\omega t}, \quad \text{(A2)}$$

where β was set to 15 min^{-1}, similarly to the periphery block, and ω was determined from cardiac output (see below) and the volume constraint.

To simulate the whole-body circulatory model, the multiexponential block impulse responses were first represented in state space form (representing multiexponential functions in the Jordan canonical form and convolution as a series arrangement). The whole-body response was then obtained by combining the heart-lung and periphery block state space representations in their feedback arrangement. The rate of glucose appearance $R_a(t)$ (tracer infusion or glucose production) was accounted for by expressing the heart-lung block inlet concentration as the sum of the periphery block outlet concentration and $R_a(t)/F$, where F is the cardiac output (dilution principle). Cardiac output was assumed to be 120 mL·kg^{-1}·min^{-1}; this value was corrected for the ratio of whole-blood to plasma glucose concentration (0.73), as glucose was measured in plasma [21]. A more complete description of the differential equations can be found in Mari et al [22].

The mean transit time of the heart-lung and periphery blocks was determined from the transit time density function of the blocks (the impulse response normalized to its areas). For the periphery block, the mean transit time is:

$$T = 1/\gamma + w_1/\lambda_1 + w_2/\lambda_2 + (1 - w_1 - w_2)/\lambda_3. \quad \text{(A3)}$$

An analogous expression applies to the heart-lung block.

Glucose clearance was calculated as $F{\cdot}E$. The volume of each block was calculated from the equation [16]:

$$V = V_R + V_{NR} = F(1 - E)T + F{\cdot}E{\cdot}\overline{T} = V_R\left(1 + \frac{E}{1 - E}\frac{\overline{T}}{T}\right), \quad \text{(A4)}$$

where the total volume V, precisely defined as the total mass at steady state normalized to arterial concentration, is expressed as the sum of 2 terms. The first term (V_R) is denoted as recirculating volume and is computable from cardiac output and the mean transit time. The second term (V_{NR}) is denoted as nonrecirculating volume because it is a fraction of the glucose mass that is removed by metabolism in the organs and does not exchange with the circulation. This term cannot be computed because it involves the artery-uptake mean transit time $\overline{T}$, which cannot be determined [16]. Therefore, the computable recirculating volume component was calculated

(adding up the heart-lung and periphery terms) and presented in the results.

REFERENCES

[1] Steele R, Wall JS, De Bodo RC, et al. Measurement of size and turnover rate of body glucose pool by the isotope dilution method. Am J Physiol 1956;187:15-24.
[2] Norwich KH. Measuring rates of appearance in systems which are not in steady state. Can J Physiol Pharmacol 1973;51:91-101.
[3] Radziuk J, Norwich KH, Vranic M. Experimental validation of measurements of glucose turnover in nonsteady state. Am J Physiol 1978;234:E84-93.
[4] Insel PA, Liljenquist JE, Tobin JD, et al. Insulin control of glucose metabolism in man. A new kinetic analysis. J Clin Invest 1975;55:1057-66.
[5] Steele R. Influences of glucose loading and of injected insulin on hepatic glucose output. Ann N Y Acad Sci 1959;82:420-30.
[6] Cobelli C, Mari A, Ferrannini E. Non-steady state\error analysis of Steele's model and developments for glucose kinetics. Am J Physiol 1987;252:E679-89.
[7] Cobelli C, Toffolo G, Ferrannini E. A model of glucose kinetics and their control by insulin, compartmental and noncompartmental approaches. Math Biosci 1984;72:291-315.
[8] Ferrannini E, Smith JD, Cobelli C, et al. Effect of insulin on the distribution and disposition of glucose in man. J Clin Invest 1985;76:357-64.
[9] Bergman RN, Steil GM, Bradley DC, et al. Modeling of insulin action in vivo. Annu Rev Physiol 1992;54:861-83.
[10] Mari A. Mathematical modeling in glucose metabolism and insulin secretion. Curr Opin Clin Nutr Metab Care 2002;5: 495-501.
[11] Norwich KH. Noncompartmental models of whole-body clearance of tracers: a review. Ann Biomed Eng 1997;25: 421-39.
[12] Hovorka R, Chassin LJ, Ellmerer M, et al. A simulation model of glucose regulation in the critically ill. Physiol Meas 2008;29: 959-78.
[13] Dassau E, Palerm CC, Zisser H, et al. In silico evaluation platform for artificial pancreatic beta-cell development—a dynamic simulator for closed-loop control with hardware-in-the-loop. Diabetes Technol Ther 2009;11:187-94.
[14] Youn JH, Kim JK, Steil GM. Assessment of extracellular glucose distribution and glucose transport activity in conscious rats. Am J Physiol 1995;268:E712-21.
[15] Steil GM, Richey J, Kim JK, et al. Extracellular glucose distribution is not altered by insulin: analysis of plasma and interstitial L-glucose kinetics. Am J Physiol 1996;271: E855-64.
[16] Mari A. Circulatory models of intact-body kinetics and their relationship with compartmental and noncompartmental analysis. J Theor Biol 1993;160:509-31.
[17] Katz A, Nyomba BL, Bogardus C. No accumulation of glucose in human skeletal muscle during euglycemic hyperinsulinemia. Am J Physiol 1988;255:E942-5.
[18] Camacho RC, Pencek RR, Lacy DB, et al. Portal venous 5-aminoimidazole-4-carboxamide-1-beta-D-ribofuranoside infusion overcomes hyperinsulinemic suppression of endogenous glucose output. Diabetes 2005;54:373-82.
[19] Issekutz Jr B. Studies on hepatic glucose cycles in normal and methylprednisolone-treated dogs. Metabolism 1977;26: 157-70.
[20] Mari A. Determination of the single-pass impulse response of the body tissues with circulatory models. IEEE Trans Biomed Eng 1995;42:304-12.
[21] McGuinness OP, Mari A. Assessment of insulin action on glucose uptake and production during a euglycemic-hyperinsulinemic clamp in dog: a new kinetic analysis. Metabolism 1997;46:1116-27.
[22] Mari A, Stojanovska L, Proietto J, et al. A circulatory model for calculating non-steady-state glucose fluxes. Validation and comparison with compartmental models. Comput Methods Programs Biomed 2003;71:269-81.
[23] DeFronzo RA, Ferrannini E. Influence of plasma glucose and insulin concentration on plasma glucose clearance in man. Diabetes 1982;31:683-8.
[24] Newsholme EA, Leech AR. Biochemistry for the medical sciences. Chichester: John Wiley & Sons; 1986.
[25] Ferrannini E, Del Prato S, DeFronzo RA. Glucose kinetics: tracer methods. In: Clarke WL, Larner J, Pohl SL, editors. Methods in diabetes research Vol II: clinical methods. New York: John Wiley & Sons; 1986. p. 107-41.
[26] Bonuccelli S, Muscelli E, Gastaldelli A, et al. Improved tolerance to sequential glucose loading (Staub-Traugott effect): size and mechanisms. Am J Physiol Endocrinol Metab 2009;297:E532-7.
[27] Mari A. Assessment of insulin sensitivity and secretion with the labeled intravenous glucose tolerance test: improved modeling analysis. Diabetologia 1998;41:1029-39.
[28] Natali A, Gastaldelli A, Camastra S, et al. Dose-response characteristics of insulin action on glucose metabolism: a non–steady-state approach. Am J Physiol Endocrinol Metab 2000;278:E794-801.